CANCER GENOMICS & PROTEOMICS *12*: 347-358 (2015)

Doxorubicin Affects Expression of Proteins of Neuronal Pathways in MCF-7 Breast Cancer Cells

MARIAN PETROVIC[1,2], CEDRIC SIMILLION[2], PETER KRUZLIAK[3], JAN SABO[1] and MANFRED HELLER[2]

[1]*Department of Medical and Clinical Biophysics, Faculty of Medicine, University of Pavol Jozef Safarik, Kosice, Slovak Republic;*
[2]*Department of Clinical Research, Proteomics and Mass Spectrometry Core Facility, University of Bern, Bern, Switzerland;*
[3]*International Clinical Research Center, St. Anne's University Hospital and Masaryk University, Brno, Czech Republic*

Abstract. *In the present article, we report on the semi-quantitative proteome analysis and related changes in protein expression of the MCF-7 breast cancer cell line following treatment with doxorubicin, using the precursor acquisition independent from ion count (PAcIFIC) mass spectrometry method. PAcIFIC represents a cost-effective and easy-to-use proteomics approach, enabling for deep proteome sequencing with minimal sample handling. The acquired proteomic data sets were searched for regulated Reactome pathways and Gene Ontology annotation terms using a new algorithm (SetRank). Using this approach, we identified pathways with significant changes (≤0.05), such as chromatin organization, DNA binding, embryo development, condensed chromosome, sequence-specific DNA binding, response to oxidative stress and response to toxin, as well as others. These sets of pathways are already well-described as being susceptible to chemotherapeutic drugs. Additionally, we found pathways related to neuron development, such as central nervous system neuron differentiation, neuron projection membrane and SNAP receptor activity. These later pathways might indicate biological mechanisms on the molecular level causing the known side-effect of doxorubicin chemotherapy, characterized as cognitive impairment, also called 'chemo brain'. Mass spectrometry data are available via ProteomeXchange with identifier PXD002998.*

Breast cancer, the most common form of cancer in women, has the second highest morbidity rate worldwide (10.9% of all cancers). It ranks as the fifth highest cause of death from any cancer, and it is still the most frequent cause of cancer-related death in women (1). Doxorubicin is a DNA-intercalating agent that has been used as an effective chemotherapeutic treatment for many types of solid tumors, including breast, lung, ovarian, prostate, and bladder (2, 3). However, its use is severely limited by side-effects such as cognitive deficits characterized as 'chemo brain' including dizziness and lack of concentration, as well as cardio-toxicity and heart failure (3).

Breast cancer research on the molecular level requires good *in vitro* models. The MCF-7 breast cancer cell line was isolated more than 50 years ago and has been widely used to study effects of anticancer drugs (4, 5). Proteomics has been applied since the onset of this millennium to reveal protein expression changes in the cytosolic, mitochondrial, cell surface, and secreted fraction of MCF-7 cells upon treatment with doxorubicin (6-9). The focus of these studies was on drug resistance. A very early study using short-term treatment with a low dose of 0.1 μM doxorubicin revealed a decrease in heat shock protein 27 (HSP27) expression (10). A decrease of HSP27 expression by 0.1 μM doxorubicin treatment was later confirmed, together with a concomitant increase in Ser-82 phosphorylation (11).

In all studies, data-dependent precursor ion selection methods were applied for protein identification. Data-dependent acquisition methods do have a major drawback in terms of dynamic range, in that the mass spectrometer triggers peptide precursor fragmentation only on the most intense signals detected during survey scans. Low-intensity peptide ions are often not detected, leading to loss of proteomic data (12). Data-independent acquisition in mass spectrometry (MS), such as precursor acquisition independent from ion count (PAcIFIC), can potentially solve this issue (13). To achieve a better dynamic range, proteome coverage and protein count, we applied the PAcIFIC method (14). The proteomic method employed herein involved a combination of PAcIFIC MS together with nano-flow liquid chromatography (LC), and semi-quantitative relative

Correspondence to: Manfred Heller, Department of Clinical Research, University of Bern, Freiburgstrasse 15, 3010 Bern, Switzerland. Tel: +41 316328404, e-mail: manfred.heller@dkf.unibe.ch

Key Words: Doxorubicin, chemotherapy, side-effects, PAcIFIC, LC-MS/MS, breast cancer, pathway analysis, chemo brain, neuronal pathway down-regulation.

protein expression analysis between treatment-naive and doxorubicin-treated breast cancer cells. The acquired proteomic data for both sample types were searched for over-represented Reactome pathways and Gene Ontology annotation terms using the newly-developed SetRank algorithm.

Materials and Methods

Cell lines and culture. MCF-7 breast cancer cells (American Type Culture Collection, Manassas, USA) were cultured and maintained in Dulbecco's modified Eagle's medium supplemented with 2 mM L-glutamine, 1 mM sodium pyruvate and 4.5 g/l glucose, 10% heat-inactivated fetal bovine serum and 1% penicillin/streptomycin (Life Technologies, purchased from LuBioScience GmbH, Lucerne, Switzerland).

Cell treatment. Cells were cultured in 75 cm^2 cell culture flasks (Becton Dickinson, New Jersey, USA) until 90% confluence by seeding at a density of 1×10^6 cells per flask. Cells were incubated in a 100% humidified atmosphere at 37˚C in the presence of 5% CO_2. Cells were washed with pre-warmed Tris-buffered saline (TBS) and treated with fresh medium in the presence or absence of 1 μM doxorubicin (Sigma Aldrich, Buchs/SG, Switzerland) for 17 h. The medium was subsequently discarded, and cells were washed 10-times with pre-warmed TBS.

Cell harvest and preparation of cell lysates. Following treatment, 1.8 ml of cold lysis buffer containing 8 M urea, 50 mM TRIS/HCl, 10 mM NaF, 2 mM Na_3VO_4 and protease inhibitor cocktail (1 tablet/10 ml lysis buffer - Roche, Rotkreuz, Switzerland), was added to the cells in the culture flask and the cells were harvested by scraping. Thereafter, the cell solution was transferred to new tubes. Cells were sonicated in an ice-water bath for 10 min. Cell debris were removed by centrifugation at 16,000 × *g* for 10 min at 4˚C, and the supernatant was transferred to a new tube. The protein concentration of the supernatant was determined using the Bradford method. Samples with a protein concentration of 1 mg/ml were reduced at 37˚C with 0.1 M dithiothreitol and alkylated at 37˚C in the dark with 0.5 M iodoacetamide. Next, reduced and alkylated proteins were precipitated by adding cold acetone (−20˚C) to a final concentration of 80% and incubated at −20˚C overnight. The protein sample was then centrifuged at 16,000 × *g* for 30 min at 4˚C. The supernatant was discarded and the pellet was washed twice with cold acetone. After washing, the protein pellet was dried in ambient air for 15 min and subsequently re-dissolved with 8 M urea and sonicated in an ice-water bath for 10 min. This solution was diluted with 20 mM TRIS/HCl, 2 mM $CaCl_2$ (pH=8) to a final urea concentration of 2 M. Proteins were digested by trypsin at a ratio of 50:1 at 37˚C overnight. Digestion was stopped by addition of 20% (v/v) trifluoroacetic acid (TFA) to a final concentration of 1%.

LC-MS/MS analysis. Peptide samples were reconstituted in water to a concentration of 100 ng/μl and 5 μl were injected in a Thermo Ultimate 3000 system onto the trapping column PepMap100 (100 Å C18, 20 mm ×75 μm ID) (Dionex, Dreieich, Germany) at a flow rate of 5 μl/min with 0.1% TFA in water. Peptides were eluted onto an analytical column (150 mm × 75 μm ID, packed with 100 Å Magic C18 material) using a flow rate of 400 nl/min as follows (%A/%B): 95:5 hold for 6 min, ramp to 60:40 over 60 min, ramp to 40:60 over 2 min, ramp to 20:80 over 1 min, hold for 5 min, ramp to 95:5 over 1 min followed by column re-equilibration under the same condition. Mobile phases A and B were water/acetonitrile at a ratio of 98:2 and 5:95, respectively, containing 0.1% (v/v) formic acid. Peptides were analyzed on a Velos LTQ iontrap (Thermo Scientific, Reinach/BL, Switzerland) using a data-independent acquisition method (PAcIFIC) (14) with the following parameters: the maximum injection time was set to 100 ms and the target ion population was 10^4. A total of 26 consecutive PAcIFIC runs were performed as follows: In the first injection, 25 MS scans with m/z isolations at 400, 401.5, 403, 404.5, 406, 407.5, 409, 410.5, 412, 413.5, 415, 416.5, 418, 419.5, 421, 422.5, 424, 425.5, 427, 428.5, 430, 431.5, 433, 434.5, 436 m/z units and an isolation width set to 2.5 Da with a relative collision energy set to 30% was repeated over the entire run. The subsequent injection covered the m/z range from 437.5 to 473.5, followed by the next injection covering the next m/z range of 36 units, etc. until m/z of 1400 was reached, 26 injections in total.

Data processing. The RAW file of each PAcIFIC run of both samples was converted to MGF files with ProteomeDiscoverer 1.4 (Thermo Scientific) entering each fragment spectrum twice with the charge state set at +2 and +3, respectively. Data were searched with EasyProt (SIB, Lausanne, Switzerland) (15) against the Uniprot_SwissProt human protein database. The precursor tolerance was set to 3.5 Da with carbamylation of cysteine as the fixed modification and oxidation of methionine as the variable. The filter criteria (double-, and triple-charged peptides) were adjusted, keeping the empirically determined protein false discovery rate (FDR) below 1.0%. The FDR is automatically calculated by EasyProt using the number of peptide spectra matches (PSM) in the reversed database divided by the number of peptides found in the forward and reversed database. Protein identifications were accepted when more than one unique peptide composed of at least six amino acids was found.

Pathway analysis. Two sets of proteins were determined. The first set consisted of proteins only observed in the treatment-naive MCF-7 culture. The second set included proteins unique to the doxorubicin-treated culture. Protein abundance was estimated semi-quantitatively based on the number of PSMs. Both protein sets were searched for over-represented Reactome pathways and Gene Ontology annotation terms using the newly-developed SetRank algorithm. Firstly, a one-tail Fisher's exact test was used to test the relative abundance of each gene set – a pathway or a term – in a set of unique proteins compared to all detected proteins over both cultures. If a gene set was significantly more abundant in a unique set with a p-value ≤0.01, it was retained. Next, false-positive hits were eliminated from the list of significant gene sets by testing for each pair of gene sets if the significance of one set was not purely the result of overlapping with the second. The full details of the SetRank algorithm will be published elsewhere.

Results

Each PAcIFIC replicate from the treatment-naive MCF-7 culture and doxorubicin-treated culture was interpreted using EasyProt (SIB, Lausanne, Switzerland) and resulted in 2,073 and 2,064 proteins with an FDR of <1%, respectively. For 197 proteins, the coverage was greater than 50%, and for a further 600, the coverage was between 20% and 50%. Over 300 proteins were identified with more than 10 unique peptides.

The acquired proteomic data sets were evaluated for over-represented Reactome pathways and Gene Ontology annotation terms applying the SetRank algorithm to proteins identified only in one condition. Tables I and II show the up- and down-regulated proteins with their gene names. In the set of proteins only recorded in doxorubicin-treated cultures, the following pathways were found to be significantly affected: embryonic development (GO:0009790) (16), sequence-specific DNA binding (GO:0043565) (17), response to oxidative stress (GO:0009636) (18), response to toxin (19), anti-oxidant activity (20), intrinsic apoptotic signaling pathway in response to DNA damage by p53 class mediator (21), as well as RNA polymerase II transcription regulatory region sequence-specific DNA binding transcription factor activity involved in positive regulation of transcription (GO:0001228) (Table I). Similarly, we were able to identify the following pathways in the set of proteins only recorded in the treatment-naive culture, *i.e.* absent from the doxorubicin-treated cultures: chromatin organization (GO:0006325) (22), DNA binding (GO:0003677) (23), condensed chromosome (GO:0000793) (24,25), cellular response to transforming growth factor beta stimulus (GO:0071560), negative regulation of response to external stimulus (GO:0032102), anatomical structure maturation (GO:0071695) and a humoral immune response (GO:0006959). Additionally, proteins of central nervous system neuron differentiation (GO:0021953), neuron projection membrane (GO:0032589) and SNAP receptor activity pathways (GO:0005484) were detected (Table II). The differentially expressed proteins belonging to each GO term are also listed in Tables III and IV, respectively.

Discussion

In the present study, we analyzed the breast cancer cell line MCF-7 with nanoLC-MS/MS using the PAcIFIC method in order to identify and quantify proteins differentially expressed in response to doxorubicin treatment. In summary, the PAcIFIC data-independent acquisition resulted in a considerable proteome coverage of MCF-7 cells without prior protein or peptide fractionation.

The high degree of protein identification and coverage enabled for protein expression and related pathway analysis, similar to a previously published study on tamoxifen-induced drug resistance in MCF-7 cells (13). The applied SetRank algorithm using a *p*-value cut-off of 0.05 identified three groups of pathways: pathways involved in direct response to intercalation of DNA, those resulting from the toxic effect of doxorubicin, and those involved in the central nervous system (Figure 1). The first two groups consisted of up- and down-regulated pathways, while the proteins of the three pathways belonging to the central nervous system were all down-regulated. The finding of up-regulated proteins of three pathways in the toxin group, response to oxidative stress, response to toxin, and anti-oxidant activity, respectively, correlated well with the known effects of doxorubicin on human metabolism (17, 18). Doxorubicin-induced oxidative stress has been well-documented, confirming our findings on up-regulation of proteins involved in oxidative stress and antioxidative activity (22, 26, 27). However, the sequence-specific DNA binding pathway is described, especially in relation to cell apoptosis (18).

The correlation between embryonic development and RNA polymerase II transcription regulatory region sequence-specific DNA binding transcription factor activity involved in positive regulation of transcription pathways, however, remains unclear. The effect of doxorubicin on these pathways was relatively well-described previously (19-21). Most interestingly, we found a set of proteins down-regulated by doxorubicin belonging to three pathways involved in central nervous system hemostasis: central nervous system neuron differentiation (GO:0021953), neuron projection membrane (GO:0032589), and SNAP receptor activity (GO:0005484). Neurons are the basic information processing structures in the central nervous system. Everything occurring above the level of neurons also qualifies as information processing. Under this light, it may be suggested that the correct equilibrium of this processing is crucial for flawless function of neuronal systems. A total of 12 proteins are members of the aforementioned pathways.

The central nervous system neuron differentiation pathway (GO:0021953) is defined as the process in which a relatively unspecialized cell acquires specialized features of a neuron whose cell body resides in the central nervous system (28). In this pathway, we identified down-regulation of homebox protein (HOXD10), myotrophin (MTPN), mitochondrial 2-oxoglutarate dehydrogenase (OGDH), eukaryotic translation initiation factor3 subunit (BHPRT1), probable E3 ubiquitin-protein ligase (MYCBP2) and microtubule-associated protein 2 (MAP2). HOXD10 is expressed in overlapping domains in the developing lumbar spinal cord and surrounding mesoderm. In mice, down-regulation of HOXD10 alters the trajectory of spinal nerves and reduces the complement of motor neurons present in the lumbar spinal cord (29, 30). MTPN protein has a potential function in cerebellar morphogenesis, and it may be involved in the differentiation of cerebellar neurons. Additionally, MTPN is highly expressed in neurons throughout the brain (31, 32). The possibility of neuron-specific MYCBP2 function has been previously hypothesized. It was suggested that two parallel MYCBP2-mediated signaling pathways regulate neuronal growth (33). The role of the other three proteins belonging to this pathway is ill-defined (inferred from electron annotations and expression patterns).

The neuron projection membrane pathway (GO:0032589) is defined as the portion of the plasma membrane surrounding a neuron projection. Three down-regulated proteins were

Table I. *Proteins up-regulated (X) after doxorubicin treatment in MCF-7 cells and corresponding GO terms.*

	GO term													
Protein ID	01228	06893	06979	09636	09790	16209	30672	32088	42771	43565	46931	50321	70008	71470
GABPA	X	-	-	-	X	-	-	-	-	X	-	-	-	-
TP53	X	-	X	X	X	-	-	-	X	-	-	-	-	-
CEBPB	X	-	-	-	X	-	-	-	-	X	-	-	-	-
FOXA1	X	-	-	-	X	-	-	-	-	X	-	-	-	-
SP1	X	-	-	-	X	-	-	-	-	X	-	-	-	-
ANK3	-	X	-	-	-	-	-	-	-	-	-	-	-	-
GOLGA4	-	X	-	-	-	-	-	-	-	-	-	-	-	-
SPTBN1	-	X	-	-	-	-	-	-	-	-	-	-	-	-
ARFRP1	-	X	-	-	X	-	-	-	-	-	-	-	-	-
MACF1	-	X	-	-	X	-	-	-	-	-	-	-	-	-
NQO1	-	-	X	X	-	X	-	-	-	-	-	-	-	-
KRT1	-	-	X	-	-	-	-	-	-	-	-	-	-	-
NUDT1	-	-	X	-	-	-	-	-	-	-	-	-	-	-
NDUFS8	-	-	X	-	-	-	-	-	-	-	-	-	-	-
PRDX5	-	-	X	-	-	X	-	-	-	-	-	-	-	-
RRM2B	-	-	X	-	-	-	-	-	-	-	-	-	-	-
NAPRT1	-	-	X	-	-	-	-	-	-	-	-	-	-	-
SRXN1	-	-	X	-	-	X	-	-	-	-	-	-	-	-
CAT	-	-	X	-	-	X	-	X	-	-	-	-	-	-
TP53I3	-	-	X	-	-	-	-	-	-	-	-	-	-	-
CCS	-	-	X	-	-	X	-	-	-	-	-	-	-	-
PML	-	-	X	-	-	-	-	-	X	-	-	-	-	-
PRKD1	-	-	X	-	-	-	-	-	-	-	-	-	-	-
PXN	-	-	X	-	-	-	-	-	-	-	-	-	-	-
HBA2	-	-	X	-	-	X	-	-	-	-	-	-	-	-
LIG1	-	-	X	-	-	-	-	-	-	-	-	-	-	-
CDK1	-	-	X	X	X	-	-	-	-	-	-	-	-	-
PRKAA1	-	-	X	-	-	-	-	-	-	-	-	X	-	-
ASNS	-	-	-	X	-	-	-	-	-	-	-	-	-	-
CDH1	-	-	-	X	X	-	-	-	-	-	-	-	-	-
CDK4	-	-	-	X	-	-	-	-	-	-	-	-	-	-
CDKN1A	-	-	-	X	-	-	-	-	-	-	-	-	-	-
MPST	-	-	-	X	-	-	-	-	-	-	-	-	-	-
SCFD1	-	-	-	X	-	-	-	-	-	-	-	-	-	-
HMGCL	-	-	-	-	X	-	-	-	-	-	-	-	-	-
SMARCA5	-	-	-	-	X	-	-	-	-	-	-	-	-	-
FOXD4L1	-	-	-	-	X	-	-	-	-	X	-	-	-	-
MSH2	-	-	-	-	X	-	-	-	X	X	-	-	-	-
SRSF1	-	-	-	-	X	-	-	-	-	-	-	-	-	-
CSDA	-	-	-	-	X	-	-	-	-	-	-	-	-	X
GNA13	-	-	-	-	X	-	-	-	-	-	-	-	-	-
PITPNB	-	-	-	-	X	-	-	-	-	-	-	-	-	-
TANC2	-	-	-	-	X	-	-	-	-	-	-	-	-	-
EPN1	-	-	-	-	X	-	-	-	-	-	-	-	-	-
MBD3	-	-	-	-	X	-	-	-	-	-	-	-	-	-
RIC8A	-	-	-	-	X	-	-	-	-	-	-	-	-	-
GRSF1	-	-	-	-	X	-	-	-	-	-	-	-	-	-
AMBRA1	-	-	-	-	X	-	-	-	-	-	-	-	-	-
PPP1R13L	-	-	-	-	X	-	-	-	-	-	-	-	-	-
MLL	-	-	-	-	X	-	-	-	-	X	-	-	-	-
POU4F3	-	-	-	-	X	-	-	-	-	X	-	-	-	-
PRKRA	-	-	-	-	X	-	-	-	-	-	-	-	-	-
RUNX2	-	-	-	-	X	-	-	-	-	-	-	-	-	-
DLG1	-	-	-	-	X	-	-	-	-	-	-	-	-	-
ALB	-	-	-	-	-	X	-	-	-	-	-	-	-	-
GSTK1	-	-	-	-	-	X	-	-	-	-	-	-	-	-

Table I. *Continued*

Table I. *Continued*

	GO term													
Protein ID	01228	06893	06979	09636	09790	16209	30672	32088	42771	43565	46931	50321	70008	71470
PRDX4	-	-	-	-	-	X	-	-	-	-	-	-	-	-
SNAPIN	-	-	-	-	-	-	X	-	-	-	-	-	-	-
DTNBP1	-	-	-	-	-	-	X	-	-	-	-	-	-	-
SLC6A17	-	-	-	-	-	-	X	-	-	-	-	-	-	-
TRIM37	-	-	-	-	-	-	-	X	-	-	-	-	-	-
RPS3	-	-	-	-	-	-	-	X	-	-	-	-	-	-
CHP1	-	-	-	-	-	-	-	X	-	-	-	-	-	-
PYCARD	-	-	-	-	-	-	-	X	X	-	-	-	-	-
SNW1	-	-	-	-	-	-	-	-	X	-	-	-	-	-
NR3C2	-	-	-	-	-	-	-	-	-	X	-	-	-	-
NFYC	-	-	-	-	-	-	-	-	-	X	-	-	-	-
ZNF24	-	-	-	-	-	-	-	-	-	X	-	-	-	-
MTA1	-	-	-	-	-	-	-	-	-	X	-	-	-	-
CTCF	-	-	-	-	-	-	-	-	-	X	-	-	-	-
ZGPAT	-	-	-	-	-	-	-	-	-	X	-	-	-	-
ARX	-	-	-	-	-	-	-	-	-	X	-	-	-	-
FOSL2	-	-	-	-	-	-	-	-	-	X	-	-	-	-
XRCC5	-	-	-	-	-	-	-	-	-	X	-	-	-	-
HNRNPD	-	-	-	-	-	-	-	-	-	X	-	-	-	-
NCL	-	-	-	-	-	-	-	-	-	X	-	-	-	-
HNRNPA2B1	-	-	-	-	-	-	-	-	-	X	-	-	-	-
NUP93	-	-	-	-	-	-	-	-	-	-	X	-	-	-
NUP153	-	-	-	-	-	-	-	-	-	-	X	-	-	-
NUP107	-	-	-	-	-	-	-	-	-	-	X	-	-	-
GSK3A	-	-	-	-	-	-	-	-	-	-	-	X	-	-
GSK3B	-	-	-	-	-	-	-	-	-	-	-	X	-	-
PREP	-	-	-	-	-	-	-	-	-	-	-	-	X	-
CTSA	-	-	-	-	-	-	-	-	-	-	-	-	X	-
SCPEP1	-	-	-	-	-	-	-	-	-	-	-	-	X	-
DDX3X	-	-	-	-	-	-	-	-	-	-	-	-	-	X
ARHGEF2	-	-	-	-	-	-	-	-	-	-	-	-	-	X

identified: myosin-1d (MYO1D), non-erythrocyte spectrin beta chain1 (SPTBN1), and dendrin (DDN). MYO1D, a necessary modulator of formation of the actin cytoskeleton in the nervous system, is expressed in developing neurons and sensory cells (34). SPTBN1, together with actin, is essential in neurons for the establishment of neuronal polarity, transport of cargos, growth of axons, and stabilization of synaptic structures (35). The exact function of DDN in the nervous system is unknown but it has been shown that this protein is up-regulated by sleep deprivation in rats (36). Additionally, dendrin interacts directly with α-actinin and membrane-associated guanylate kinase with inverted orientation/ synaptic scaffolding molecule, which are contained in the postsynaptic cytoskeleton (37).

Proteins exhibiting SNAP receptor activity (GO:0005484) act as a marker identifying a membrane and interact selectively with one or more soluble *N*-ethylmaleimide-sensitive factor attachment protein receptors (SNAREs) on another membrane to mediate membrane fusion. The SNAP protein family belongs to the SNARE complex, that is, among other things, active as a neuromediator. We identified, according to these pathways, a down-regulation of syntaxin-16 (STX16), SNAP29 and STX17 proteins.

SNARE proteins, such as the STX protein family (STX12, STX13) play crucial roles in neurons. STX16 is specifically enriched in neuronal dendrites and found at Golgi outposts. In addition, STX16 may play a role in neurite out-growth and perhaps other specific dendritic anterograde/retrograde traffic (38-40). On the other hand, the function of STX16 was specifically required for, and restricted to, the retrograde pathway in trans-Golgi network/Golgi membranes of neurons (41). STX17 is a divergent member of the syntaxin family of SNARE proteins and was identified in human carcinoma cell lines (42). Our findings regarding down-regulation of these proteins could indicate inhibition of these processes in the central nervous system (Figure 2).

Table II. *Proteins down-regulated (X) after doxorubicin treatment of MCF-7 cells and corresponding GO terms.*

	GO term									
Protein ID	0000793	0003677	0005484	0006325	0006959	0021953	0032102	0032589	0071560	0071695
AKAP8	X	X	-	-	-	-	-	-	-	-
CTCF	X	X	-	X	-	-	-	-	-	-
PES1	X	-	-	-	-	-	-	-	-	-
H2AFX	X	X	-	X	-	-	-	-	-	-
MKI67IP	X	-	-	-	-	-	-	-	-	-
CSNK1A1	X	-	-	-	-	-	-	-	-	-
PPP1CC	X	-	-	-	-	-	-	-	X	-
BUB3	X	-	-	-	-	-	-	-	-	-
NDE1	X	-	-	-	-	-	-	-	-	-
ERCC6L	X	X	-	-	-	-	-	-	-	-
SPC25	X	-	-	-	-	-	-	-	-	-
SPC24	X	-	-	-	-	-	-	-	-	-
NUP43	X	-	-	-	-	-	-	-	-	-
LIG3	X	X	-	-	-	-	-	-	-	-
NSMCE2	X	-	-	-	-	-	-	-	-	-
PARP1	-	X	-	-	-	-	-	-	X	-
BCL3	-	X	-	-	X	-	-	-	-	-
CCNT1	-	X	-	-	-	-	-	-	X	-
DDX3X	-	X	-	-	-	-	-	-	-	-
DNA2	-	X	-	-	-	-	-	-	-	-
ENO1	-	X	-	-	-	-	-	-	-	-
GATA3	-	X	-	X	X	-	X	-	-	X
GTF2A1	-	X	-	-	-	-	-	-	-	-
H1F0	-	X	-	X	-	-	-	-	-	-
HIST1H1E	-	X	-	X	-	-	-	-	-	-
HIST1H1B	-	X	-	X	-	-	-	-	-	-
HMGN1	-	X	-	X	-	-	-	-	-	-
AGFG1	-	X	-	-	-	-	-	-	-	-
MCM3	-	X	-	-	-	-	-	-	-	-
NFYB	-	X	-	-	-	-	-	-	-	-
PBX1	-	X	-	-	-	-	-	-	-	-
POLR2C	-	X	-	-	-	-	-	-	-	-
MAPK1	-	X	-	-	-	-	-	-	-	-
RFC2	-	X	-	-	-	-	-	-	-	-
RPL6	-	X	-	-	-	-	-	-	-	-
SMARCA1	-	X	-	X	-	-	-	-	-	-
SMARCC1	-	X	-	X	-	-	-	-	-	-
SP100	-	X	-	-	-	-	-	-	-	-
SURF6	-	X	-	-	-	-	-	-	-	-
XRCC5	-	X	-	-	-	-	-	-	-	-
BRPF1	-	X	-	X	-	-	-	-	-	-
DEK	-	X	-	X	-	-	-	-	-	-
KDM5D	-	X	-	X	-	-	-	-	-	-
ARID1A	-	X	-	X	-	-	-	-	-	-
HIST2H2AC	-	X	-	X	-	-	-	-	-	-
NCOR2	-	X	-	-	-	-	-	-	X	-
BCLAF1	-	X	-	-	-	-	-	-	-	-
TOX4	-	X	-	-	-	-	-	-	-	-
SRA1	-	X	-	-	-	-	-	-	-	-
HUWE1	-	X	-	X	-	-	-	-	-	-
PQBP1	-	X	-	-	-	-	-	-	-	-
SRRM1	-	X	-	-	-	-	-	-	-	-
KDM5B	-	X	-	X	-	-	-	-	-	-
WDHD1	-	X	-	X	-	-	-	-	-	-
AKAP8L	-	X	-	-	-	-	-	-	-	-
NUSAP1	-	X	-	-	-	-	-	-	-	-
ZFR	-	X	-	-	-	-	-	-	-	-
PBRM1	-	X	-	X	-	-	-	-	-	-
NKRF	-	X	-	-	-	-	-	-	-	-
KIF15	-	X	-	-	-	-	-	-	-	-
PRDM15	-	X	-	-	-	-	-	-	-	-
ZFP2	-	X	-	-	-	-	-	-	-	-
TTC5	-	X	-	-	-	-	-	-	-	-

Table II. *Continued*

Table II. *Continued*

	GO term									
Protein ID	0000793	0003677	0005484	0006325	0006959	0021953	0032102	0032589	0071560	0071695
C17orf49	-	X	-	X	-	-	-	-	-	-
ZBTB9	-	X	-	-	-	-	-	-	-	-
HIST2H2AB	-	X	-	X	-	-	-	-	-	-
YY2	-	X	-	-	-	-	-	-	-	-
HIST2H3D	-	X	-	X	-	-	-	-	-	-
RFX8	-	X	-	-	-	-	-	-	-	-
CREB1	-	X	-	-	-	-	-	-	-	-
PRDX5	-	X	-	-	-	-	-	-	-	-
RPS3	-	X	-	-	-	-	-	-	-	-
PNKP	-	X	-	-	-	-	-	-	-	-
PURB	-	X	-	-	-	-	-	-	-	-
CSDA	-	X	-	-	-	-	-	-	-	-
NABP2	-	X	-	-	-	-	-	-	-	-
HNRNPD	-	X	-	-	-	-	-	-	-	-
NCL	-	X	-	-	-	-	-	-	-	-
TAF2	-	X	-	-	-	-	-	-	-	-
TAF7	-	X	-	X	-	-	-	-	-	-
MTA2	-	X	-	X	-	-	-	-	-	-
HNRNPA2B1	-	X	-	-	-	-	-	-	-	-
HOXC11	-	X	-	-	-	-	-	-	-	-
HOXD10	-	X	-	-	-	X	-	-	-	-
ALX1	-	X	-	-	-	-	-	-	-	-
MYBBP1A	-	X	-	-	-	-	-	-	-	-
VSX1	-	X	-	-	-	-	-	-	-	-
POLE4	-	X	-	X	-	-	-	-	-	-
STX16	-	-	X	-	-	-	-	-	-	-
SNAP29	-	-	X	-	-	-	-	-	-	-
STX17	-	-	X	-	-	-	-	-	-	-
TLK1	-	-	-	X	-	-	-	-	-	-
HIRIP3	-	-	-	X	-	-	-	-	-	-
ASF1B	-	-	-	X	-	-	-	-	-	-
ACTL6A	-	-	-	X	-	-	-	-	-	-
SUPT4H1	-	-	-	X	-	-	-	-	-	-
LEO1	-	-	-	X	-	-	-	-	-	-
MRGBP	-	-	-	X	-	-	-	-	-	-
UTP3	-	-	-	X	-	-	-	-	-	-
SRPK1	-	-	-	X	-	-	-	-	-	-
BRD8	-	-	-	X	-	-	-	-	-	-
PRMT5	-	-	-	X	-	-	-	-	-	-
PYGO2	-	-	-	X	-	-	-	-	-	-
SNW1	-	-	-	X	-	-	-	-	X	-
GPI	-	-	-	-	X	-	-	-	-	-
KRT1	-	-	-	-	X	-	-	-	-	-
C3	-	-	-	-	X	-	-	-	-	-
MTPN	-	-	-	-	-	X	-	-	-	-
OGDH	-	-	-	-	-	X	-	-	-	-
HPRT1	-	-	-	-	-	X	-	-	-	-
MYCBP2	-	-	-	-	-	X	-	-	-	-
MAP2	-	-	-	-	-	X	-	-	-	-
ANXA1	-	-	-	-	-	-	X	-	-	-
RYK	-	-	-	-	-	-	X	-	-	-
UACA	-	-	-	-	-	-	X	-	-	-
CD276	-	-	-	-	-	-	X	-	-	-
CTNNA2	-	-	-	-	-	-	X	-	-	-
MYO1D	-	-	-	-	-	-	-	X	-	-
SPTBN1	-	-	-	-	-	-	-	X	-	-
DDN	-	-	-	-	-	-	-	X	-	-
LIMS1	-	-	-	-	-	-	-	-	X	-
RHOA	-	-	-	-	-	-	-	-	X	X
LTBP2	-	-	-	-	-	-	-	-	X	-
PPM1A	-	-	-	-	-	-	-	-	X	-
PPP1CB	-	-	-	-	-	-	-	-	X	-
UBA52	-	-	-	-	-	-	-	-	X	-
SNX6	-	-	-	-	-	-	-	-	X	-
ANKRD17	-	-	-	-	-	-	-	-	-	X

Table III. *Summary of statistical evaluation of pathways with proteins up-regulated by doxorubicin treatment in MCF-7 cells.*

GO Term	Description	Database	*p*-Value	pp	Number of proteins in the pathway	Number of significant proteins in the pathway	*p*-Value	
							Corrected	Adjusted
06979	Response to oxidative stress	BP	0.001559029	2.80714575	53	19	0.001559029	0.021826409
01228	RNA polymerase II transcription regulatory region sequence-specific DNA binding transcription factor activity involved in positive regulation of transcription	MF	0.002971602	2.527009425	7	5	0.002971602	0.03863082
09636	Response to toxin	BP	0.003311684	2.479951053	19	9	0.003311684	0.038707165
43565	Sequence-specific DNA binding	MF	0.003225597	2.491389881	60	20	0.003225597	0.038707165
06893	Golgi to plasma membrane transport	BP	0.006745375	2.170993924	8	5	0.006745375	0.059915984
09790	Embryonic development	BP	0.007401595	2.130674699	103	29	0.007401595	0.059915984
16209	Antioxidant activity	MF	0.007473486	2.126476755	21	9	0.007473486	0.059915984
30672	Synaptic vesicle membrane	CC	0.005991598	2.222457304	3	3	0.005991598	0.059915984
32088	Negative regulation of NF-κB transcription factor activity	BP	0.006745375	2.170993924	8	5	0.006745375	0.059915984
42771	Intrinsic apoptotic signaling pathway in response to DNA damage by p53 class mediator	BP	0.006745375	2.170993924	8	5	0.006745375	0.059915984
46931	Pore complex assembly	BP	0.005991598	2.222457304	3	3	0.005991598	0.059915984
50321	Tau-protein kinase activity	MF	0.005991598	2.222457304	3	3	0.005991598	0.059915984
70008	Serine-type exopeptidase activity	MF	0.005991598	2.222457304	3	3	0.005991598	0.059915984
71470	Cellular response to osmotic stress	BP	0.005991598	2.222457304	3	3	0.005991598	0.059915984

BP, Biological process; MF, molecular function; CC, cellular component.

In a previous proteomic study dealing with the influence of doxorubicin on MCF-7 cells, a set of proteins involved in the neuron central system was identified as cathepsin D (43-45). Another study demonstrated the differentiation of neuronal markers of MCF-7 cells, such as nestin, tubulin beta-3 chain (TUBB3) and glial fibrillary acidic protein (GFAP) (46). We can state that it is very likely that if these proteins are not expressed by MCF-7 cells after treatment with doxorubicin, the same may occur in neuronal cells treated with doxorubicin. Proteins involved in pathways that are crucial to brain function, disappear upon treatment with doxorubicin, and this likely explains the development of post-chemotherapy cognitive impairment symptoms in patients, also called 'chemo brain' (Figure 2).

Conflicts of Interest

The Authors declare no conflicts of interest.

Acknowledgements

Marian Petrovic was supported by the Sciex-NMS grant from the Conference of Rectors of Universities of Switzerland (CRUS). This study was elaborated within the grant of the European Regional Development Fund—Project FNUSA-ICRC (No. CZ.1.05/1.1.00/02.0123) and the Swiss National Science Foundation for LC-MS instrument funding (R'Equip project #316030-139231). The mass spectrometry proteomics data have been deposited to the ProteomeXchange Consortium (47) *via* the PRIDE partner repository with the dataset identifier PXD002998.

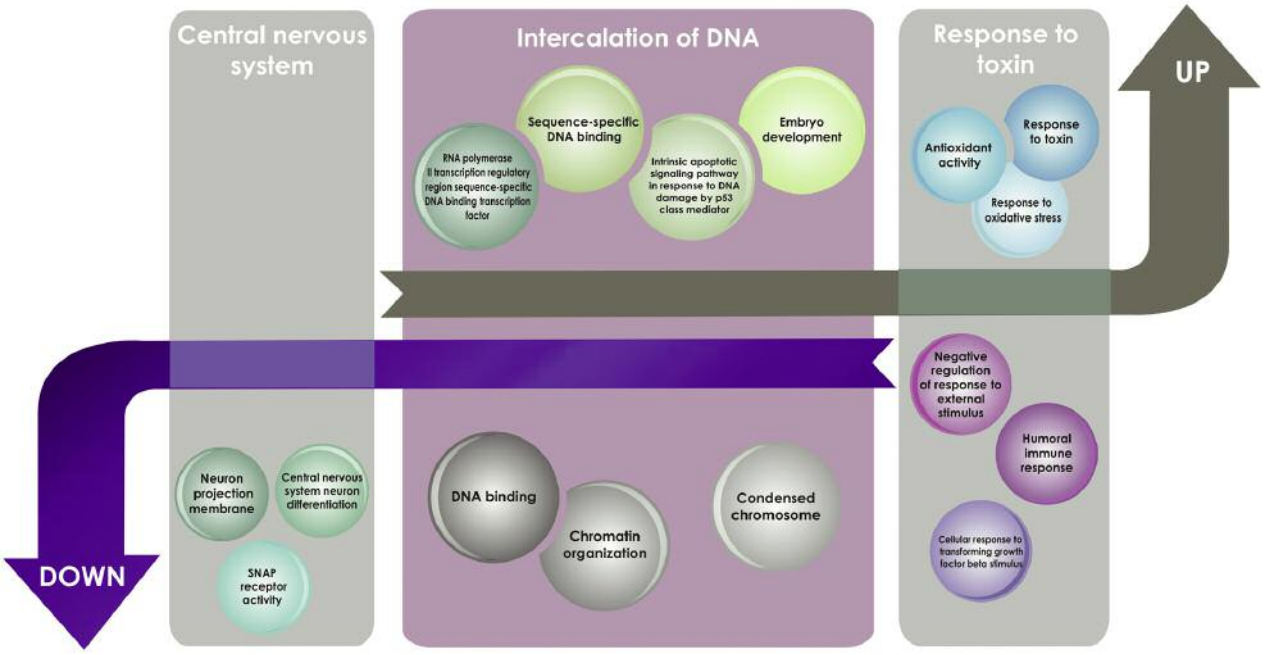

Figure 1. *Pathways where proteins were found to be up- or down-regulated after doxorubicin treatment on MCF-7 cells.*

Table IV. *Summary of statistical evaluation of pathways with proteins down regulated on doxorubicin treatment of MCF-7 cells.*

GO Term	Description	Database	*p*-Value	pp	Number of proteins in the pathway	Number of significant proteins in the pathway	*p*-Value	
							Corrected	Adjusted
0003677	DNA binding	MF	8.4E-05	4.0734931	289	78	8.4432E-05	0.00084432
0006325	Chromatin organization	BP	0.00053	3.2788897	120	37	0.000526151	0.004735357
0032102	Negative regulation of response to external stimulus	BP	0.00076	3.1166024	8	6	0.000764535	0.006116284
0000793	Condensed chromosome	CC	0.0093	2.0315173	44	15	0.009299994	0.04370898
0005484	SNAP receptor activity	MF	0.00624	2.2045274	3	3	0.00624414	0.04370898
G0006959	Humoral immune response	BP	0.00717	2.1442287	8	5	0.007174164	0.04370898
0021953	Central nervous system neuron differentiation	BP	0.00762	2.118013	11	6	0.007620563	0.04370898
0032589	Neuron projection membrane	CC	0.00624	2.2045274	3	3	0.00624414	0.04370898
0071560	Cellular response to transforming growth factor beta stimulus	BP	0.0063	2.2003227	31	12	0.006304887	0.04370898
0071695	Anatomical structure maturation	BP	0.00624	2.2045274	3	3	0.00624414	0.04370898

BP, Biological process; MF, molecular function; CC, cellular component.

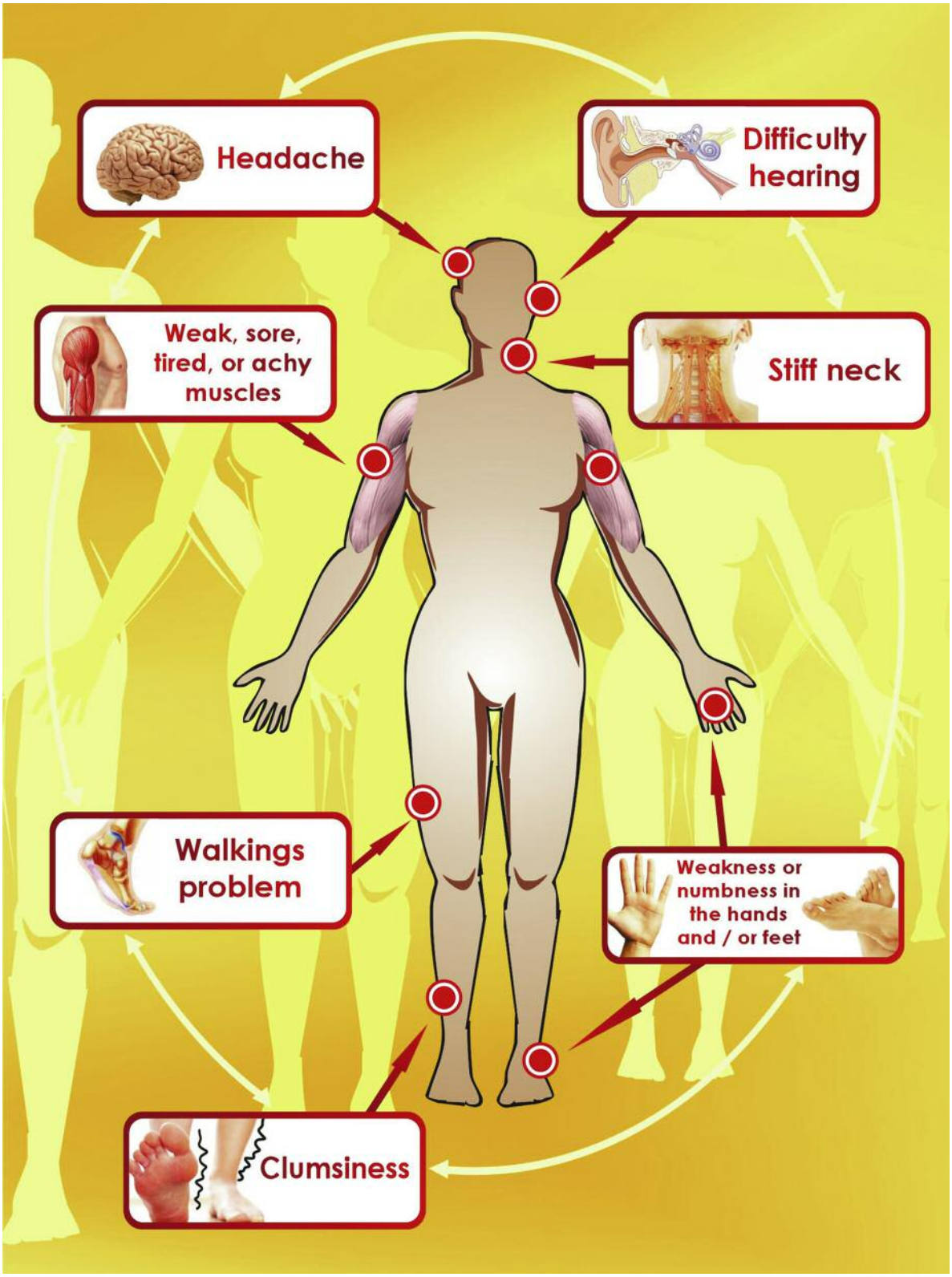

Figure 2. *Side-effects of 'chemo brain'. The phenomenon 'chemo brain' refers to a cluster of cognitive deficiencies, which are caused by systemic cancer treatment. The main features of 'chemo brain' include headache, difficulty in hearing, stiff neck, weakness, walking problems, muscle problems, and deficits in attention, memory, reaction time, speed of information, judgment, and planning.*

References

1 Gangopadhyay S, Nandy A, Hor P and Mukhopadhyay A: Breast cancer stem cells: a novel therapeutic target. Clin Breast Cancer *13*: 7-15, 2013.

2 Zhang N, Klegerman ME, Deng H, Shi Y, Golunski and An Z: Trastuzumab-doxorubicin conjugate provides enhanced anti-cancer potency and reduced cardiotoxicity. J Cancer Ther *4*: 308-322, 2013.

3 Evans AR, Miriyala S, St Clair DK, Butterfield DA and Robinson RA: Global effects of adriamycin treatment on mouse splenic protein levels. J Proteome Res *11*: 1054-1064, 2012.

4 Soule HD, Vazquez J, Long A, Albert S, Brennan M: A human cell line from a pleural effusion derived from a breast carcinoma. J Nat Cancer Inst *51*: 1409-1416, 1973.

5 Comşa Ş, Cîmpean AM and Raica M: The Story of MCF-7 Breast Cancer Cell Line: 40 years of Experience in Research. Anticancer Res *35*: 3147-3154, 2015.

6 Wang Z, Liang S, Lian X, Liu L, Zhao S, Xuan Q, Guo L, Liu H, Yang Y, Dong T, Liu Y, Liu Z and Zhang Q: Identification of proteins responsible for adriamycin resistance in breast cancer cells using proteomics analysis. Sci Rep 5: 9301, 2015.

7 Strong R, Nakanishi T, Ross D and Fenselau C: Alterations in the mitochondrial proteome of adriamycin resistant MCF-7 breast cancer cells. J Proteome Res *5*: 2389-2395, 2006.

8 Yao L, Zhang Y, Chen K, Hu X and Xu LX: Discovery of IL-18 as a novel secreted protein contributing to doxorubicin resistance by comparative secretome analysis of MCF-7 and MCF-7/Dox. PLoS One *6*: e24684, 2011.

9 Balashova EE, Dashtiev MI and Lokhov PG: Proteomic footprinting of drug-treated cancer cells as a measure of cellular vaccine efficacy for the prevention of cancer recurrence. Mol Cell Proteomics *11*: M111.014480, 2012.

10 Chen ST, Pan TL, Tsai YC and Huang C: Proteomics reveals protein profile changes in doxorubicin – treated MCF-7 human breast cancer cells. Cancer Lett *181*: 95-107, 2002.

11 Xu F, Yang T, Fang D, Xu Q and Chen Y: An investigation of heat shock protein 27 and P-glycoprotein mediated multi-drug resistance in breast cancer using liquid chromatography-tandem mass spectrometry-based targeted proteomics. J Proteomics *108*: 188-197, 2014.

12 Panchaud A, Scherl A, Shaffer SA, von Haller PD, Kulasekara HD, Miller SI and Goodlett DR: PAcIFIC: How to dive deeper into the proteomics ocean. Anal Chem *81*: 6481-6488, 2009.

13 Hengel SM, Murray E, Langdon S, Hayward L, O'Donoghue J, Panchaud A, Hupp T and Goodlett DR: Data-independent proteomic screen identifies novel tamoxifen agonist that mediates drug resistance. J Proteome Res *10*: 4567-4578, 2011.

14 Scherl A, Shaffer SA, Taylor GK, Kulasekara HD, Miller SI and Goodlett DR: Genome-specific gas-phase fractionation strategy for improved shotgun proteomic profiling of proteotypic peptides. Anal Chem *80*: 1182-1191, 2008.

15 Gluck F, Hoogland C, Antinori P, Robin X, Nikitin F, Zufferey A, Pasquarello C, Fétaud V, Dayon L, Müller M, Lisacek F, Geiser L, Hochstrasser D, Sanchez JC and Scherl A: EasyProt - An easy-to-use graphical platform for proteomics data analysis. J Proteomics *79*: 146-160, 2013.

16 Wang QL, Sun SC, Han J, Kwak YC, Kim NH and Cui XS: Doxorubicin induces early embryo apoptosis by inhibiting poly(ADP ribose) polymerase. In Vivo *26*: 827-834, 2012.

17 Wei L, Surma M, Gough G, Shi S, Lambert-Cheatham N, Chang J and Shi J: Dissecting the Mechanisms of Doxorubicin and Oxidative Stress-Induced Cytotoxicity: The Involvement of Actin Cytoskeleton and ROCK1. PLoS ONE *10*: e0131763, 2015.

18 El-Sayed EM, Mansour AM and Abdul-Hameed MS: Thymol and Carvacrol Prevent Doxorubicin-Induced Cardiotoxicity by Abrogation of Oxidative Stress, Inflammation, and Apoptosis in Rats. J. Biochem. Mol. Toxicol Epub ahead of print, 2015.

19 Antberg L, Cifani P, Levander F and James P: Pathway-centric analysis of the DNA damage response to chemotherapeutic agents in two breast cell lines. EuPA Open Proteomics *8*: 128-136, 2015.

20 Himmetoglu S, Dincer Y, Ersoy YE, Bayraktar B, Celik V and Akcay T: DNA oxidation and antioxidant status in breast cancer. J Investig Med *57*: 720-723, 2009.

21 Uji K, Naoi Y, Kagara N, Shimoda M, Shimomura A, Maruyama N, Shimazu K, Kim SJ and Noguchi S: Significance of TP53 mutations determined by next-generation "deep" sequencing in prognosis of estrogen receptor-positive breast cancer. Cancer Lett *342*: 19-26, 2014.

22 Zunino F, Di Marco A, Zaccara A and Gambetta RA: The interaction of daunorubicin and doxorubicin with DNA and chromatin. Biochim Biophys Acta *607*: 206-214, 1980.

23 Mencalha A, Victorino VJ, Cecchini R and Panis C: Mapping Oxidative Changes in Breast Cancer: Understanding the Basic to Reach the Clinics. Anticancer Res *34*: 1127-1140, 2014.

24 Sen S, Hittelman WN, Teeter LD and Kuo MT: Model for the formation of double minutes from prematurely condensed chromosomes of replicating micronuclei in drug-treated Chinese hamster ovary cells undergoing DNA amplification. Cancer Res *49*: 6731-6737, 1989.

25 Hittelman WN and Rao PN: The nature of adriamycin-induced cytotoxicity in Chinese hamster cells as revealed by premature chromosome condensation. Cancer Res *35*: 3027-3035, 1975.

26 Pieniążek A, Czepas J, Piasecka-Zelga J, Gwoździński K and Koceva-Chyła A: Oxidative stress induced in rat liver by anticancer drugs doxorubicin, paclitaxel and docetaxel. Adv Med Sci *58*: 104-111, 2013.

27 Deavall DG, Martin EA, Horner JM and Roberts R: Drug-induced oxidative stress and toxicity. J Toxicol *2012*: 645460, 2012.

28 Qiang L, Inoue K and Abeliovich A: Instant neurons directed somatic cell reprogramming models of central nervous system disorders. Biol Psychiatry *75*: 945-951, 2014.

29 Lin AW and Carpenter EM: Hoxa10 and Hoxd10 coordinately regulate lumbar motor neuron patterning. J Neurobiol *56*: 328-337, 2003.

30 Philippidou P and Dasen JS: Hox Genes: Choreographers in Neural Development, Architects of Circuit Organization. Neuron *80*: 12-34, 2013.

31 Krek A, Grün D, Poy MN, Wolf R, Rosenberg L, Epstein EJ, MacMenamin P, da Piedade I, Gunsalus KC, Stoffel M and Rajewsky N: Combinatorial microRNA target predictions. Nat Genet *37*: 495-500, 2005.

32 Fujigasaki H, Song SY, Kobayashi T and Yamakuni T: Murine central neurons express a novel member of the CDC10/SWI6 motif-containing protein superfamily. Mol Brain Res *40*: 203-213, 1996.

33 Holland S and Scholich K: Regulation of neuronal functions by the E3-ubiquitinligase protein associated with MYC (MYCBP2). Commun Integr Biol *4*: 513-515, 2011.
34 Kneussel M and Wagner W: Myosin motors at neuronal synapses: drivers of membrane transport and actin dynamics. Nat Rev Neurosci *14*: 233-247, 2013.
35 Cingolani LA and Goda Y: Actin in action: the interplay between the actin cytoskeleton and synaptic efficacy. Nat Rev Neurosci. *9*: 344-356, 2008.
36 Neuner-Jehle M, Denizot JP, Borbély AA and Mallet J: Characterization and sleep deprivation-induced expression modulation of dendrin, a novel dendritic protein in rat brain neurons. J Neurosci Res *46*: 138-151, 1996.
37 Kremerskothen J, Kindler S, Finger I, Veltel S and Barnekow A: Postsynaptic recruitment of Dendrin depends on both dendritic mRNA transport and synaptic anchoring. J Neurochem *96*: 1659-1666, 2006.
38 Chua CE and Tang BL: Syntaxin 16 is enriched in neuronal dendrites and may have a role in neurite outgrowth. Mol Membr Biol *25*: 35-45, 2008.
39 Wang Y, Tai G, Lu L, Johannes L, Hong W and Tang BL: Trans-Golgi network syntaxin 10 functions distinctly from syntaxins 6 and 16. Mol Membr Biol *4*: 313-325, 2005.
40 Simonsen A, Bremnes B, Rønning E, Aasland R and Stenmark H: Syntaxin-16, a putative Golgi t-SNARE. Eur J Cell Biol *75*: 223-231, 1998.
41 Abascal-Palacios G, Schindler C, Rojas AL, Bonifacino JS and Hierro A: Structural Basis for the Interaction of the Golgi-Associated Retrograde Protein Complex with the t-SNARE Syntaxin 6. Structure *21*: 1698-1706, 2013.
42 Zhang Q, Li J, Deavers M, Abbruzzese JL and Ho L: The subcellular localization of syntaxin 17 varies among different cell types and is altered in some malignant cells. J Histochem Cytochem *53*: 1371-1382, 2005.
43 Chen ST, Pan TL, Tsai YC and Huang CM: Proteomics reveals protein profile changes in doxorubicin-treated MCF-7 human breast cancer cells. Cancer Lett *181*: 95-107, 2002.
44 Amritraj A, Wang Y, Revett TJ, Vergote D, Westaway D and Kar S: Role of cathepsin D in U18666A-induced neuronal cell death: potential implication in Niemann-Pick type C disease pathogenesis. J Biol Chem *288*: 3136-3152, 2012.
45 Leong S, Nunez AC, Lin MZ, Crossett B, Christopherson RI and Baxter RC: iTRAQ-based proteomic profiling of breast cancer cell response to doxorubicin and TRAIL. J Proteome Res *11*: 3561-3572, 2006.
46 Zhang Q, Fan H, Shen J, Hoffman RM and Xing HR: Human breast cancer cell lines co-express neuronal, epithelial, and melanocytic differentiation markers *in vitro* and *in vivo*. PLoS ONE *5*: e9712, 2010.
47 Vizcaino JA, Deutsch EW, Wang R, Csordas A, Reisinger F, Rios D, Dianes JA, Sun Z, Farrah T, Bandeira N, Binz PA, Xenarios I, Elsenacher M, Mayer G, Gatto L, Campos A, Chalkley RJ, Kraus HJ, Albar JP, Martinez-Bartolomés S, Apweiler R, Omenn GS, Martens L, Jones AR and Hermjakob H: ProteomeXchange provides globally co-ordinated proteomics data submission and dissemination. Nat Biotechnol *30*: 223-226, 2014.

Received September 3, 2015
Revised October 9, 2015
Accepted October 19, 2015